# The Characterization of Soft Antifriction Coating on the Tin Bronze by Electro-spark Alloying

**Zhengchuan ZHANG [1], Ievgen KONOPLIANCHENKO [1], Viacheslav TARELNYK [1] *, Guanjun LIU [2], Xin DU [1], Hua YU [3]**

[1] *Technical Services Department, Sumy National Agrarian University, H. Kondratiieva str. 160, Sumy, 40021, Ukraine*
[2] *School of Mechanical and Electrical Engineering, Henan Institute of Science and Technology, Hualan str. 90, Xinxiang, 453000, China*
[3] *School of Material Science and Engineering, Henan University of Science and Technology, Kaiyuan str. 263, Luoyang, 471003, China*

crossref http://dx.doi.org/10.5755/j02.ms.30610

*Received 01 February 2022; accepted 12 May 2022*

Soft materials such as silver, copper and Babbitt SnSb11Cu6 were deposited on the surface of tin bronze by electro spark alloying (ESA) to form the antifriction coating. The data of the antifriction coating were tested by electronic balance, three-dimensional optical profilometer, scanning electron microscope (SEM), energy dispersive spectrometer (EDS), X-ray diffractometer (XRD), Vickers microhardness tester and tribometer. The mass gain, roughness, thickness, surface morphology and phase composition, cross-section and element distribution, microhardness and tribological properties of the antifriction coating were analyzed. The results show that the grain size of the antifriction coating is fine and the metallurgical bonding between the coating and the substrate is good. The surface of each substrate is composed of three layers of coating. The optimal parameters of electro spark alloying are as follows: the discharge voltages of Ag, Cu and Babbitt alloy coatings are 60 V, 60 V and 30 V respectively, the energy storage capacitance is 150 μF, 150 μF and 90 μF respectively, and the working efficiency is 3 min/cm$^2$, 3 min/cm$^2$ and 4 min/cm$^2$ respectively. Under the optimized parameters, the average mass transfer efficiency is 54.4 mg/cm$^2$, the average surface roughness is 32.3 μm, and the maximum thickness is about 160 μm. The surface friction coefficient of the soft antifriction coating is 55.6 % of that of the tin bronze substrate. The main wear mechanisms of the soft antifriction coating prepared by electro spark alloying technique are plastic deformation accompanied by slight polishing.
*Keywords:* electro spark alloying, antifriction coating, phase composition, element distribution, friction.

## 1. INTRODUCTION

Electro spark alloying (ESA) is a kind of surface treatment technology which uses periodic electric pulse energy to melt the electrode material as an anode and deposit it on the surface of another material to form a special functional coating [1 – 3]. The output energy of electro spark alloying is low, and few electrode materials are melted by single pulse discharge, so the electrode materials are quickly cooled and solidified after being deposited on the substrate, the grains are refined, the ultrafine grains are generated, even the amorphous coating is generated, and the performance of the functional coating can be changed more abundantly [4 – 6]. The main advantage of ESA is that it can change various properties of material surfaces [7, 8], the metallurgical bonding strength between the coating and the substrate is high, and the deposited coating is compact [9, 10]. The pulse duration is short, very little heat is transferred to the workpiece, the temperature change of the substrate is small, and almost no deformation occurs [11 – 13]. With the advantages of small size, easy operation and low cost, ESA has become one of the most promising surface treatment methods in the field of surface engineering [14 – 16].

The gas turbine works under the conditions of heavy load, high speed and high temperature, but it will also be affected by the corrosive and abrasive working environment. Usually, the surface layer bears the largest load and is most affected by the external environment, so the surface performance directly determines the working life and stability of parts. The bearing material of the gas turbine should have appropriate hardness and plasticity, low friction coefficient, strong fatigue resistance, high thermal stability, corrosion resistance, wear resistance, low cost, and the ability to store lubricating oil. Because of its excellent mechanical properties and thermal conductivity, copper-based alloy bearing is widely used. However, the analysis of their operation shows that the friction coefficient of bronze bearing is relatively large, which is easy to wear the shaft, and its tribological characteristics become an obstacle to its further application. Therefore, the electro spark alloying technology can be used to build a functional coating for the copper-based alloy bearing to improve the tribological properties, improve the surface properties, wear resistance and fatigue resistance of the bearing, and improve the reliability and durability of the bearing. However, up to now, there are few reports on specific research in this area.

In this paper, a new method of electro spark alloying is put forward to improve the friction performance of tin

*Corresponding author. Tel.: +38-0542-787640; fax: +38-0542-787640.
E-mail address: *tarelnik@i.ua* (V. Tarelnyk)

bronze by alloying soft antifriction material on the surface of tin bronze. The feasibility and technical characteristics of electro spark alloying on the surface of QS10-1 tin bronze was studied by using silver, copper and Babbitt alloy electrodes.

## 2. MATERIALS AND METHODS

### 2.1. The substrate and electrodes materials

The substrate material is tin bronze QSn10-1 (Sn 9.38 %, P 0.72 %, impurity 0.80 %, the rest is Cu) commonly used bearing material provided by Zhejiang Shenfa Bearing Co., LTD. The material QSn10-1 was cut into 29 mm × 25 mm × 4 mm by electro-spark CNC wire-cutting machine DK77-40.

Tin bronze is a relatively good thermal conductivity material, as the bearing material can quickly dissipate the heat generated by friction, which is conducive to improving the thermal stability and durability of the bearing [17, 18]. However, the tribological properties of tin bronze are limited in some applications. Tin-based Babbitt alloy has a good embedded, anti-seizure, compliance, widely used in large mechanical spindle bearings and bushings [19, 20]. Babbitt alloy has good wear resistance, but with the development of mechanical equipment towards heavy load, high speed and large-scale direction, Babbitt alloy has some shortcomings in the working process, such as high temperature softening, low speed heavy load lubrication failure, high speed variable load deformation and so on. The Babbitt alloy is alloyed on the surface of the tin bronze by the electro spark, has good friction and wear performance of the Babbitt alloy, can bear a high load, has good comprehensive mechanical property and strong applicability. The interfacial bonding strength between tin bronze and soft antifriction materials directly affects the properties of composite materials, so it is required that Babbitt alloy and tin bronze matrix must be closely bonded.

To improve the bonding strength between the substrate and Babbitt alloy, the method of using pure tin as the interlayer metal is usually used, which relies on the diffusion of the substrate and pure tin to form a transition layer to ensure the close bonding between the substrate and Babbitt alloy, but the bonding strength is often not good enough. The interfacial bonding between metals is very complex. The interfacial reaction, chemical bonding and geometric characteristics of the interface are important means to understand the relationship between the properties of composites and the bonding interface. The properties of the transition layer in bimetal composites depend on the characteristics of the two bonding metals, the chemical composition, the ability of mutual diffusion during solidification and the thermal conditions.

The wetting angle is the angle between the liquid-solid interface and the tangent line of the liquid surface at the contact point of the liquid phase and the solid phase. Electro spark alloying technology plays a dominant role in the element transition between electrode and substrate because of its high and violent metallurgical reaction temperature. But that transition of the two elements is related to a wetting angle, the small the wetting angle between the electrode material and the substrate is, the higher the dilution of the electrode material is, so that the elements of the electrode material and the element of the substrate are mutually diffused and infiltrated, a metallurgical bonding is formed in a transition layer, and the bonding strength is improved. In the process of electro spark alloying, there is an element transition between electrode and substrate. The smaller the wetting angle is, the closer the metallurgical bonding between the deposit and the substrate is, but if the dilution is too high, the proportion of electrode material to the substrate will be too large to ensure that the deposit can also have the performance of electrode material. Therefore, it is necessary to reduce the dilution and ensure the quality of the deposited layer by reducing the single pulse energy and accelerating the deposition rate. If the performance of a deposit is excellent, but the wetting angle between the electrode material and the substrate is too large, which leads to a poor density of the deposit, obvious stratification with the substrate and many cracks in the deposit, the intermediate layer can be selected.

Soft metallic silver is sometimes used in high load and high-speed bearings because of its mechanical properties, corrosion resistance and lubricating properties [21]. The wetting angle between silver and copper is relatively small, which is beneficial to strengthening the metallurgical bonding force between the coatings and is suitable for being used as a transition coating. Soft metal copper can form ε-phase ($Cu_6Sn_5$) with tin in tin-based Babbitt alloy, which is also conducive to improving the bonding force between coatings, and is also suitable for the transition layer [22 – 24]. Therefore, the surface of tin bronze is first alloyed with silver by electro spark, then with copper coating, and finally with Babbitt alloy, so that the hardness of the material is gradually reduced, which is also conducive to reducing cracks on the surface of the material. The surface of each sample is composed of three layers of coating.

The electro spark alloying electrode material is silver (99.99 %), copper (99.99 %) and Babbitt SnSb11Cu6 (B83, Sb 11.02 %, Cu 5.83 %, impurity 0.05 %, the rest is Sn), the diameter is 3 mm.

The surface of the substrate is ground and polished by the Rotary swing gravity grinding and polishing machine ZYP300.

Before coatings deposition, the substrates were cleaned in anhydrous ethanol with an ultrasonic cleaning machine for 20 minutes to remove the oil and impurities on the surface. The substrate was dried with a hairdryer in room temperature mode, and then the weight of the substrate was weighed by an electronic balance.

### 2.2. Electro spark alloying parameters

The electrode and the workpiece are kept at an angle of about 45 degrees and swing from side to side with an amplitude of about 25 mm. Travel speed in both cases was 2 mm/s. And that discharge power is gradually reduced from large to small until the thickness and the surface roughness of the coating meet the requirements. The discharge frequency increases gradually, the discharge frequency of the first layer is 3000 Hz, the discharge frequency of the second layer is 4000 Hz, and the discharge rate of the third layer is 5000 Hz. The alloying process was carried out at room temperature using a hand-held operation

with argon (99 %) as a shielding gas at a flow rate of 0.17 L/s to prevent the coating area from being affected by air.

Based on a previous experimental study, the electro spark alloying parameters (alloyed electrode, discharge voltage, energy storage capacitance, and discharge efficiency) are shown in Table 1.

**Table 1.** The ESA parameters of soft antifriction coatings

| Specimens | Electrodes | Voltage, V | Capacitance, μF | Efficiency, min/cm$^2$ |
|---|---|---|---|---|
| 1# | Ag-Cu-B83 | 40/40/20 | 90/90/30 | 1/1/2 |
| 2# | Ag-Cu-B83 | 40/40/20 | 150/150/90 | 2/2/3 |
| 3# | Ag-Cu-B83 | 40/40/20 | 240/240/150 | 3/3/4 |
| 4# | Ag-Cu-B83 | 60/60/30 | 90/90/30 | 2/2/3 |
| 5# | Ag-Cu-B83 | 60/60/30 | 150/150/90 | 3/3/4 |
| 6# | Ag-Cu-B83 | 60/60/30 | 240/240/150 | 1/1/2 |
| 7# | Ag-Cu-B83 | 50/50/25 | 90/90/30 | 3/3/4 |
| 8# | Ag-Cu-B83 | 50/50/25 | 150/150/90 | 1/1/2 |
| 9# | Ag-Cu-B83 | 50/50/25 | 240/240/150 | 2/2/3 |

## 2.3. Properties investigation

A small piece of soft antifriction coating sample is cut and embedded in that phenolic resin, and is ground, polished, cleaned, and then corroded by using 4 % of nitric acid alcohol to test the cross-section data of the soft antifriction coating.

A METTLER TOLEDO AL204 electronic balance was used to accurately measure the mass variation of the sample with an accuracy of 0.1 mg.

The surface roughness of the soft antifriction coating was measured by Bruker Contour GT-k1 three-dimensional optical profiler. The surface morphology of the soft antifriction coating was observed by scanning electron microscopy (SEM) of FEI Quanta 200. The element distribution from the coating surface to the substrate was detected by scanning electron microscopy (SEM) with an energy dispersive spectrometer (EDS).

The phase distribution data of the soft antifriction coating surface were detected by Bruker X-ray diffractometer D8 Advance A25, and the data were compared and analyzed by Jade software to determine the phase composition of the coating surface.

The microhardness distribution of the coating section was measured by VHL-VMH-002V microhardness tester. The microhardness of that soft antifriction coating was measured at different locations using an indenter with a pressure of 0.098 N and a dwell time of 12 s.

MWF-500 friction and wear tester were used to study the friction performance of the thickest coating surface. The friction data of reciprocating running of ball-plate test of the coating under the condition of dry friction at 25 °C are detected. Corresponding friction pairs are made of bearing steel (GCr15) balls with a diameter of 8 mm. A sliding speed of 20 mm/s, a pressure loading speed of 10 mm/min and a frictional contact distance of 6 mm were selected. The applied pressures were 5 N, 10 N and 15 N respectively, and the test time was 600 s each time.

## 3. RESULTS AND ANALYSIS

In Table 2, the characteristic data of the mass of the antifriction coating, the surface roughness and the coating thickness are given. The coating mass is calculated by measuring the mass of the sample before and after ESA with the electronic balance, and then the mass is divided by the coating area to obtain the coating mass per unit area, which is the value of the mass transfer. The data analysis shows that the discharge voltage has the greatest influence on the mass transfer of the soft antifriction coating, followed by the working efficiency, and finally the energy storage capacitor. When the discharge voltage is 60 V, 60 V and 30 V, the energy storage capacitance is 150 μF, 150 μF and 90 μF, the deposition efficiency is 3 min/cm$^2$, 3 min/cm$^2$ and 4 min/cm$^2$. The maximum mass increase of the soft antifriction coating is 54.4 mg/cm$^2$. Under these process parameters, the average surface roughness of the soft antifriction coating is 32.3 μm, and the maximum thickness of the soft antifriction coating is about 160 μm.

It is found that the discharge voltage has the greatest impact on the coating thickness, and the capacitance has the smallest impact on the coating thickness. When the voltage is 60 V, 60 V and 30 V, the capacitance is 150 μF, 150 μF and 90 μF, and the specific efficiency is 3 min/cm$^2$, 3 min/cm$^2$ and 4 min/cm$^2$, respectively, the optimal coating thickness is 160 μm.

In this paper, the commonly used coating evaluation methods are used, and the thickness of the coating is used as the main basis to evaluate the quality of the coating, so the optimal process parameters of soft antifriction coating on tin bronze surface by electro spark alloying are obtained. The process parameters of a silver layer are the discharge voltage 60 V, the energy storage capacitance 150 μF, and the working efficiency 3 min/cm$^2$. The process parameters of a copper layer are the discharge voltage 60 V, the energy storage capacitance 150 μF, and the working efficiency 3 min/cm$^2$. The process parameters of Babbitt layer are the discharge voltage 30 V, the energy storage capacitance 90 μF, and the working efficiency 4 min/cm$^2$.

**Table 2.** The characteristics of soft antifriction coatings

| Specimens | Electrodes | Mass transfer, mg/cm$^2$ | Roughness $R_a$, μm | Thickness, μm |
|---|---|---|---|---|
| 1# | Ag-Cu-B83 | 11.5 | 14.8 | 50 |
| 2# | Ag-Cu-B83 | 10.2 | 13.5 | 60 |
| 3# | Ag-Cu-B83 | 12.7 | 26.3 | 50 |
| 4# | Ag-Cu-B83 | 34.1 | 32.6 | 160 |
| 5# | Ag-Cu-B83 | 54.4 | 32.3 | 160 |
| 6# | Ag-Cu-B83 | 16.2 | 36.6 | 60 |
| 7# | Ag-Cu-B83 | 23.9 | 23.5 | 100 |
| 8# | Ag-Cu-B83 | 10.0 | 20.0 | 60 |
| 9# | Ag-Cu-B83 | 15.4 | 31.2 | 60 |

### 3.1. The morphology and phase composition of the soft antifriction coating surface

It can be seen from the surface microstructure of the soft anti-friction coating in Fig. 1 that the surface of the anti-friction coating is formed by the gradual accumulation of small droplets of metal electrodes melted by discharge pulse output energy. During the process of electro spark alloying, the metal surface is heated and cooled rapidly, and the residual thermal stress exists in the coating, which may cause micro-cracks on the surface. The soft metal with a low modulus ratio has good plasticity, which is beneficial to relieve the thermal stress and inhibit the generation of cracks.

And that surface of the soft antifriction coating after the

electro spark alloying can meet the requirement of the surface roughness of a bearing Bush only by simple grinding. The soft antifriction coating is beneficial to the storage of abrasive particles and the adsorption of lubricating oil on the surface of the bearing Bush, thereby reducing the damage of abrasive particles to the surface of the bearing bush, reducing the friction coefficient and improving the tribological performance [25 – 27]. The surface of the soft antifriction coating prepared by electro spark alloying has a trace of black substance which is produced by oxidation of Babbitt alloy at high temperature.

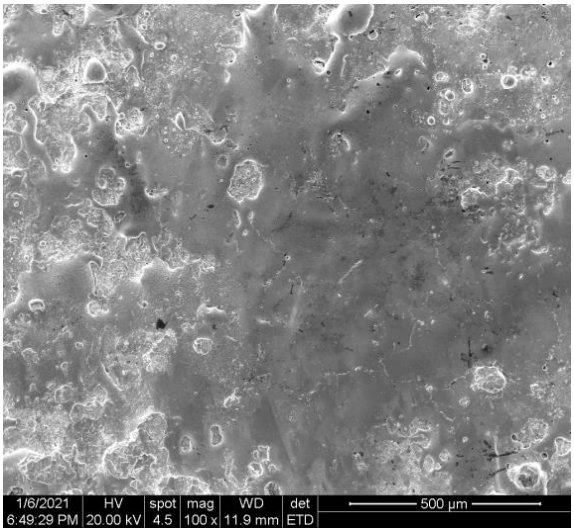


**Fig. 1.** The morphology of soft antifriction coating surface

The surface of the soft coating was sanded with 1000 grit sandpaper, and the surface of the coating was analyzed by X-ray diffraction. Fig. 2 is the X-ray diffraction pattern of the soft antifriction coating, the phase of the soft antifriction coating is obviously changed compared with that of the matrix, and the diffraction peaks mainly comprise phases of Sn, SbSn, $Cu_6Sn_5$ and Cu.

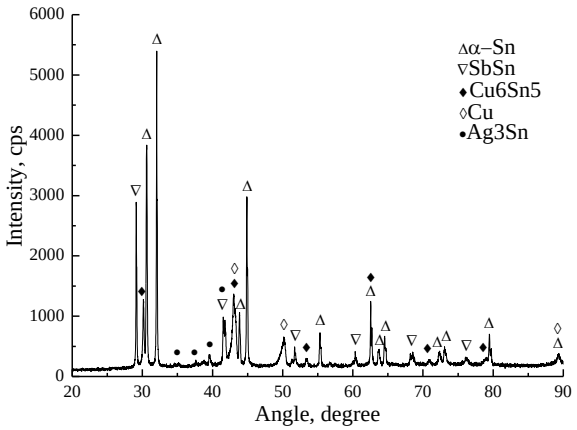


**Fig. 2.** The X-ray diffraction pattern of soft antifriction coating surface

The Sn phase exhibits strong diffraction intensity and the content of Sn in the soft antifriction coating is high. In addition, $Ag_3Sn$ phase appears in the soft antifriction coating, which indicates that under the action of high temperature and high pressure generated by electric spark discharge, silver element and tin element react to form the $Ag_3Sn$ hard phase, which is beneficial to ensuring the metallurgical bonding between metals and improving the mechanical and wear resistance properties of the workpiece surface [28]. No oxide phase, nitride phase and carbide phase were observed in the X-ray diffraction pattern, indicating that the air had little effect on the coating due to the quarantine effect of the argon atmosphere.

### 3.2. Microstructure and EDS analysis of cross-section of the soft antifriction coating

The cross-section structure of the electro spark alloying soft antifriction coating is shown in Fig. 3 a. The coating is relatively uniform and continuous, the internal structure is refined and dense, which is due to the rapid heating and cooling of the electrode and substrate by ESA technology.

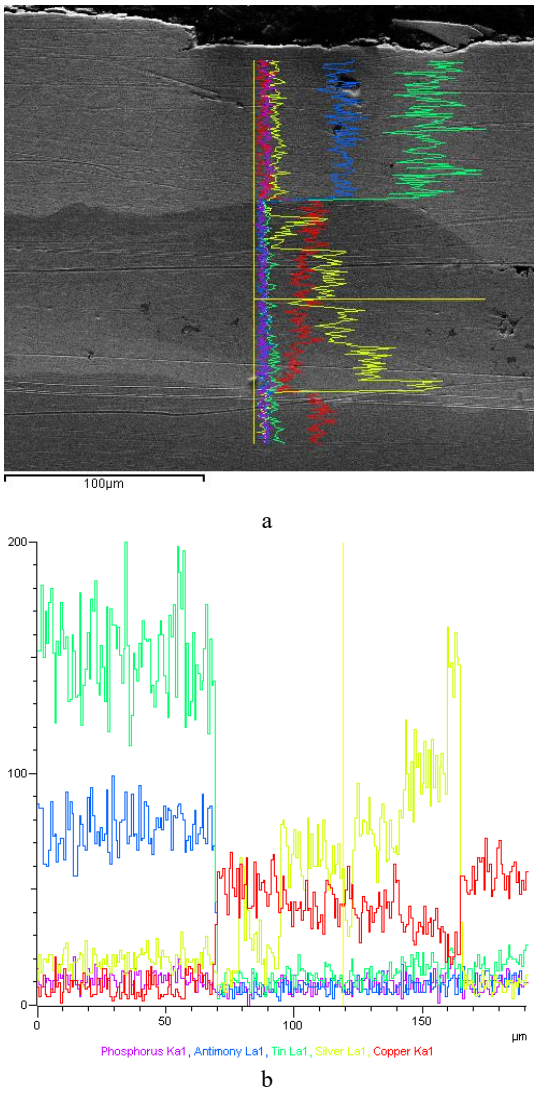


**Fig. 3.** The cross-section elemental composition of the soft antifriction coating: a – cross-section micro-morphology; b – The elemental composition of line scanning

The metallurgical bonding with the substrate is tight, and the transition layer at the interface is obvious, but there are some defects such as micro-cracks and holes in some places. The soft antifriction coatings are Babbitt B83, copper and silver from the surface to the substrate. However, because the wettability of silver and copper is very good, the silver coating can rarely be observed and the coating is completely fused during the electro spark alloying, forming

the alloy layer. Since the ESA is a process of continuous superposition of the deposited materials, the thickness of the deposited layer increases with the increase of the electrode materials deposited on the surface. During ESA, the instantaneous high temperature generated by high frequency pulse discharge melts and vaporizes the materials in the discharge area, and melts, diffuses and alloys occur on the deposited surface. Then the substrate surface is rapidly cooled and solidified, resulting in large cyclic thermal stress and microstructure stress in the deposited layer, resulting in micro-cracks or pores on the surface of the deposition. In the process of layer by layer covering, a small number of micro-cracks or pores on the surface of the coating cannot be completely filled by the molten material, forming holes.

The elemental composition of the soft antifriction coating-substrate cross-section was analyzed by EDS line scanning and the results are shown in Fig. 3 b. From the surface of the soft antifriction coating to the substrate, the content of the copper element is relatively low at first, suddenly increases at about 70 μm, then gradually decreases at 120 μm, and increases again at about 160 μm and maintains a relatively high content. This is because the initial Babbitt layer has a relatively low copper content, with a copper transition layer at about 70 μm to 120 μm, followed by a silver transition layer, and possibly the substrate after 160 μm. From the surface of the soft antifriction coating to the substrate, the content of silver element is relatively low at the beginning, gradually increases after 70 μm, is relatively high from 120 μm to 160 μm, and remains at a very low level after 160 μm. This is because the electro spark alloying violent reaction causes the Babbitt alloy coating also to contain a few elements. And that copper transition layer with excellent wettability and silver also contains a large amount of silver element. At about 120 μm to 160 μm is the silver transition layer, and then the substrate. From the surface of the soft antifriction coating to the substrate, the content of tin and antimony starts relatively high, decreases abruptly at about 70 um and remains low. The content of phosphorus has been relatively low, and the change is not easy to distinguish. In addition, no oxygen element was detected from the surface of the soft antifriction coating to the substrate, and the inner part of the coating was not oxidized, which was consistent with the XRD measurement results.

This shows that the workpiece substrate is mainly composed of elements such as copper and tin, Babbitt alloy coating is mainly composed of elements such as tin and antimony, and the intermediate layer is composed of silver and copper. The thickness of the Babbitt alloy coating is about 70 μm, the thickness of the copper coating is about 50 μm, and the thickness of the silver coating is about 40 μm. And that the total thickness of the soft antifriction coating is about 160 μm. In the process of electro spark alloying, the molten synthetic material and electrode material are infiltrated and transferred to each other, and an alloyed and metallurgically bonded micro-transition region is formed at the interface. In the transition region, there is a gradual slope of elemental content. The diffusion is mainly carried out by the vacancy mechanism [29]. The matrix or the coating and the molten electrode material form a pair of diffusion couples, the element atoms contained in the two sides diffuse to each other through the interface, and the generated intermetallic compound is uniformly distributed in the interface reaction layer. Liquid metal atoms rely on Brownian motion to collide with each other to obtain energy and diffuse into each other's surface, some external metal atoms with higher energy continue to collide with them and diffuse inward, thus occupying the vacancies left by the atoms and diffusing inward layer by layer [30].

### 3.3. Tribological properties of the soft antifriction coating

The surface microhardness of the soft antifriction coating is about 29 $HV_{0.01}$, which is 82 % lower than that of the tin bronze substrate (161 $HV_{0.01}$).

Fig. 4 compares the evolution of the friction coefficient variation during uncoating of the tin bronze tests at loads of 5 N, 10 N and 15 N.

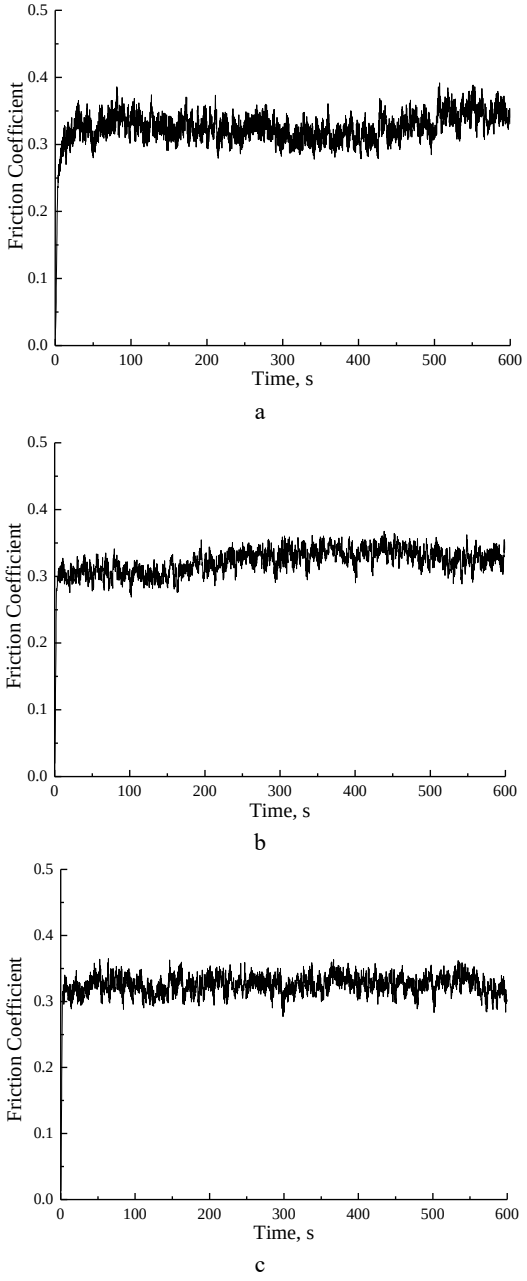


**Fig. 4.** Friction coefficient variation during uncoating of the tin bronze tests at loads: a – 5 N; b – 10 N; c – 15 N

For the initial 600 seconds at a load of 5 N, the friction

coefficient with an average value of about 0.333. In the following 600 seconds at a load of 10 N, the friction coefficient is about 0.330. And then to 15 N for the final 600 seconds, the friction coefficient is about 0.324.

Fig. 5 compares the evolution of the coefficient of friction at the applied load with 5 N, 10 N and 15 N of the ESA modified samples sliding against a GCr15 steel ball in the air.

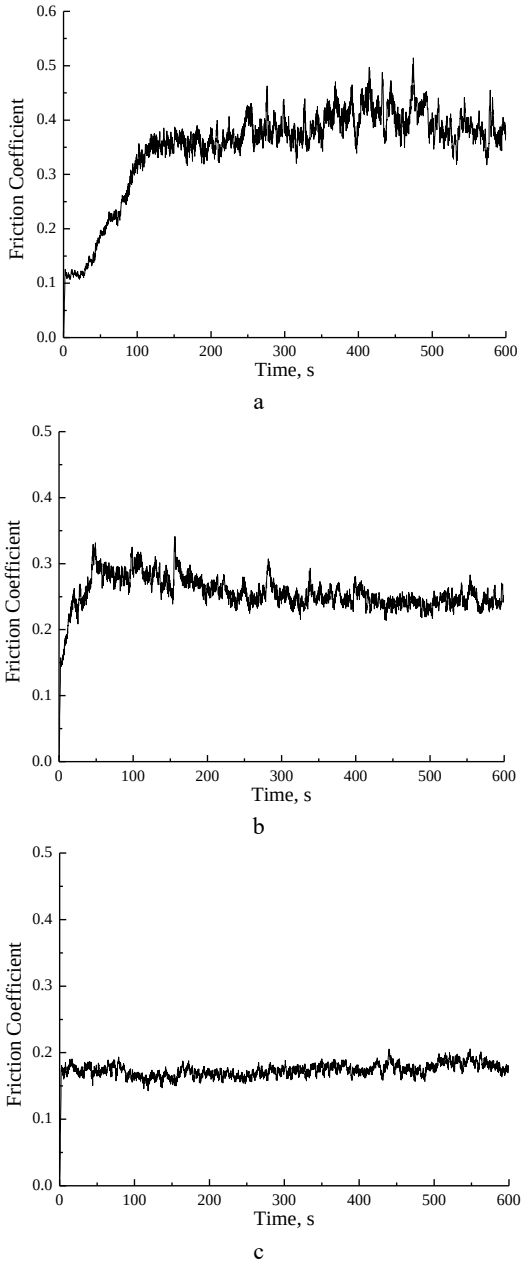


**Fig. 5.** Friction coefficient variation during antifriction coating tests at loads: a – 5 N; b – 10 N; c – 15 N

For the initial 600 seconds at a load of 5 N, the friction coefficient with an average value of about 0.399. In the following 600 seconds at a load of 10 N, the friction coefficient is about 0.244. And then to 15 N for the final 600 seconds, the friction coefficient is approximately 0.180. The investigation of the tribological properties of the coating in dry friction shows that the lower resistance is exhibited by the antifriction coatings deposited using the soft antifriction material. The surface friction coefficient of the antifriction coating is 55.6 % of the tin-bronze substrate. For the ESA layer, the friction coefficient is larger at the beginning of friction, which is mainly affected by the surface roughness. So, for the initial 600 seconds at a load of 5 N, the friction coefficient is about 0.399 influenced by the surface roughness (Fig. 5 a). Because GCr15 with higher hardness makes the soft antifriction coating with lower hardness produce plastic deformation. With the formation of the friction film, the tribological track of the soft antifriction coating-GCr15 friction pair is transferred to the surface. Similar to other common friction elements, the steady-state friction coefficient is no longer affected by the surface roughness of the friction element.

After the first running-in stage, the soft antifriction coating demonstrated a relatively stable friction coefficient with an average value of about 0.244 after the following 600 seconds at a load of 10 N (Fig. 5 b), after which it decreased to the level of 0.180 at a load of 15 N (Fig. 5 c). After that running-in stage, the friction coefficient of the soft antifriction coating keeps stable gradually.

To study the friction and wear mechanism of soft antifriction coating, the friction and wear tracks were analyzed. After the tribological performance test, the friction and wear trajectories of tin bronze and soft antifriction coating are shown in Fig. 6.

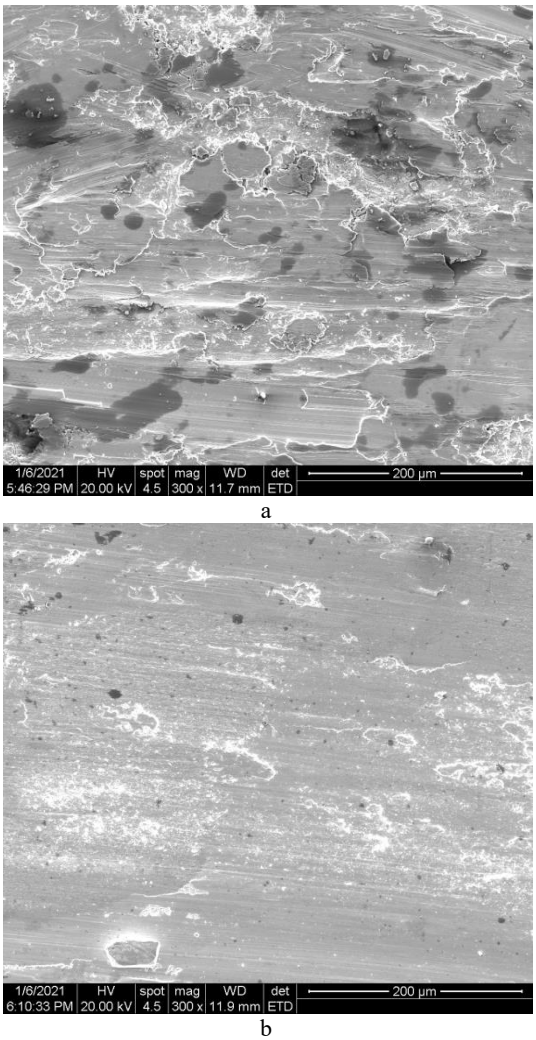


**Fig. 6.** The wear scars of the tin-bronze substrate with and without antifriction coating after tribological testing: a – Tin bronze; b – Tin-bronze with the antifriction coating

From the analysis of the friction and wear track of tin bronze in Fig. 6 a, it is found that the wear mechanism of tin bronze is mainly serious adhesive wear and ploughing wear, accompanied by plastic deformation. In the process of friction and wear, the surface of tin bronze first deforms elastically under the action of external force, then deforms plastically, and finally local fracture falls off, which becomes the third body in the process of friction and wear. The particles that broke off hardened under pressure and debris typically gets rolled over, creating additional damage. There are many wear forms on the wear surface. The grooves on the worn surface of tin bronze are mainly caused by ploughing wear, and the delamination on the worn surface is mainly caused by adhesive wear, and plastic deformation also exists. Generally speaking, the lamellar structure of the worn surface of tin bronze is conducive to reducing the friction coefficient, but the relatively large lamellar structure and ploughing also increase the surface roughness, which limits the further reduction of the friction coefficient.

But as can be seen from Fig. 6 b, no delamination is found in that the friction and wear track of the soft antifriction coating, and the main wear mechanism are plastic deformation and light polishing. Plastic deformation plays a major role in the low friction coefficient of the soft antifriction coating [31]. In the gradual running-in process, the micro-morphology of the soft anti-friction coating surface changed, the surface became smooth, there were small abrasive particles and shallow scratches, and the friction and wear tended to be stable.

## 4. CONCLUSIONS

The following conclusions can be drawn from the test results and analysis:

1. The soft antifriction coatings of silver, copper and Babbitt were deposited on the surface of tin-bronze by electro spark alloying. Under the optimal process parameters, the mass transfer is 54.4 mg/cm$^2$, the surface roughness of the antifriction coating is 32.3 μm and the maximum thickness is 160 μm. In particular, the coating obtained under the optimal process parameters is dense, grains refined, uniformly distributed and metallurgical fusion with the substrate.
2. The X-ray diffractogram patterns observed for soft antifriction coating surface indicate the phases of Sn, SbSn, $Cu_6Sn_5$ and Cu. Moreover, in the case of antifriction coating in addition a phase of $Ag_3Sn$ is appeared which is conducive to ensuring the metal bonding of the coatings.
3. The surface friction coefficient of the antifriction coating (0.180) is 55.6 % of the tin-bronze substrate (0.324). The wear mechanism of tin bronze is mainly serious adhesive wear and ploughing wear, accompanied by plastic deformation. No delamination is found in that friction and wear track of the soft antifriction coating, and the main wear mechanism is plastic deformation accompanied by light polishing.


### *Acknowledgments*

The research was funded by the Ministry of Education and Science of Ukraine (0116U002756) and the Joint Foundation of Henan Province, China (U1804142).


### REFERENCES


1. **Han, H., Guo, J., Jiao, W.** Discharge Mechanism of Electro-spark Deposition with Rotary Electrode *Transactions of the China Welding Institution* 40 (5) 2019: pp. 67 – 72. https://doi.org/10.12073/j.hjxb.2019400129
2. **Huang, Q., Chen, Z., Wei, X., Wang, L., Hou, Z., Yang, W.** Effects of Pulse Energy on Microstructure and Properties of Mo2FeB2- based Ceramet Coatings Prepared by Electro-spark Deposition *China Surface Engineering* 30 (3) 2017: pp. 89 – 96. https://doi.org/10.11933/j.issn.1007-9289.20170106002
3. **Anisimov, E., Khan, A.K., Ojo, O.A.** Analysis of Microstructure in Electro-Spark Deposited IN718 Superalloy *Materials Characterization* 119 2016: pp. 233 – 240. https://doi.org/10.1016/j.matchar.2016.07.025
4. **Kiryukhantsev-Korneev, P.V., Sheveyko, A.N., Shvindina, N.V., Levashov, E.A., Shtansky, D.V.** Comparative Study of Ti-C-Ni-Al, Ti-C-Ni-Fe and Ti-C-Ni-Al/Ti-C-Ni-Fe Coatings Produced by Magnetron Sputtering, Electro-Spark Deposition and a Combined Two-Step Process *Ceramics International* 44 (7) 2018: pp. 7637 – 7646. https://doi.org/10.1016/j.ceramint.2018.01.187
5. **Enrique, P.D., Jiao, Z., Zhou, N.Y., Toyserkani, E.** Dendritic Coarsening Model for Rapid Solidification of Ni-Superalloy Via Electrospark Deposition *Journal of Materials Processing Technology* 258 2018: pp. 138 – 143. https://doi.org/10.1016/j.jmatprotec.2018.03.023
6. **Salmaliyan, M., Ghaeni, F.M., Ebrahimnia, M.** Effect of Electro Spark Deposition Process Parameters on WC-Co Coating on H13 Steel *Surface and Coatings Technology* 321 2017: pp. 81 – 89. https://doi.org/10.1016/j.surfcoat.2017.04.040
7. **Wang, L., Cao, G., Ma, X.** Preparation of NiCrAlY Coating Electro-Spark Deposited on GH4169 Alloy *Transactions of the China Welding Institution* 38 (7) 2017: pp. 104 – 108. https://doi.org/10.12073/j.hjxb.20150917001
8. **Geng, M., Wang, W., Zhang, X.** Microstructures and Properties of Ni/Ti(C,N) Composite Cermet Coating Prepared by Electrospark Deposition *Surface Technology* 49 (4) 2020: pp. 222 – 229. https://doi.org/10.16490/j.cnki.issn.1001-3660.2020.04.025
9. **Zhang, J., Zhang, L., Liu, H.** Microstructure and Degradability of Aluminum Alloy Repaired by Electro-spark Deposition *Surface Technology* 49 (10) 2020: pp. 224 – 232. https://doi.org/10.16490/j.cnki.issn.1001-3660.2020.10.025
10. **Xu, A., Wang, X., Zhao, Y., Zhu, S., Han, G.** Experiments on ESD-Heating Remelting, Rolling Dressing *China Mechanical Engineering* 31 (14) 2020: pp. 1741 – 1746. https://doi.org/10.3969/j.issn.1004-132X.2020.14.014
11. **Yu, H., Lin, Y., Chen, C.** Research on the Character of NiCr Coating Deposited on 35CrMo Steel by the Electro-Spark Deposition *Surface Technology* 39 (4) 2010: pp. 5 – 7. https://doi.org/10.16490/j.cnki.issn.1001-3660.2010.04.014

12. **Pliszka, I., Radek, N.** Corrosion Resistance of WC-Cu Coatings Produced by Electrospark Deposition *Procedia Engineering* 192 2017: pp. 707 – 712. https://doi.org/10.1016/j.proeng.2017.06.122
13. **Padgurskas, J., Kreivaitis, R., Rukuiža, R., Mihailov, V., Agafii, V., Kriūkienė, R., Baltušnikas, A.** Tribological Properties of Coatings Obtained by Electro-Spark Alloying C45 Steel Surfaces *Surface and Coatings Technology* 311 2017: pp. 90 – 97. https://doi.org/10.1016/j.surfcoat.2016.12.098
14. **Penyashki, T., Kostadinov, G., Mortev, I., Dimitrova, E.** Investigation of Properties and Wear of WC, TiC and TiN Based Multilayer Coatings Applied onto Steels C45, 210CR12 and HS6-5-2 Deposited by Non-Contact Electrospark Process *Journal of the Balkan Tribological Association* 23 (2) 2017: pp. 325 – 342.
15. **Xiang, H., Ke, F., Tan, Y.F., Wang, X.L., Hua, T.** Effects of Process Parameters on Microstructure and Wear Resistance of TiN Coatings Deposited on TC11 Titanium Alloy by Electrospark Deposition *Transactions of Nonferrous Metals Society of China* 27 (8) 2017: pp. 1767 – 1776. https://doi.org/10.1016/S1003-6326(17)60199-7
16. **Tarelnyk, V.B., Paustovskii, A.V., Tkachenko, Y.G., Konoplianchenko, E.V., Martsynkovskyi, V.S., Antoszewski, B.** Electrode Materials for Composite and Multilayer Electrospark-Deposited Coatings from Ni–Cr and WC–Co Alloys and Metals *Powder Metallurgy and Metal Ceramics* 55 (9) 2017: pp. 585 – 595. https://doi.org/10.1007/s11106-017-9843-2
17. **Tarel'nik, V.B., Konoplyanchenko, E.V., Kosenko, P.V., Martsinkovskii, V.S.** Problems and Solutions in Renovation of the Rotors of Screw Compressors by Combined Technologies *Chemical and Petroleum Engineering* 53 (7) 2017: pp. 540 – 546. https://doi.org/10.1007/s10556-017-0378-7
18. **Chen, Y., Yu, M., Cao, K.** Advance on Copper-based Self-lubricating Coatings *Surface Technology* 50 (2) 2021: pp. 91 – 100. https://doi.org/10.16490/j.cnki.issn.1001-3660.2021.02.010
19. **Hao, Y., Wang, J., Yang, P.** Microstructures and Properties of Tin-Based Babbitt Metal Prepared by Laser Cladding Deposition *Chinese Journal of Lasers* 47 (8) 2020: pp. 1 – 10. https://doi.org/10.3788/CJL202047.0802009
20. **Song, Z., Peng, Z., Yan, M.** Effect of Fabrication Methods on Microstructures and Mechanical Properties of Tin-based Babbitt Bearings *Chinese Journal of Rare Metals* 38 (6) 2019: pp. 283 – 289. https://doi.org/10.13373/j.cnki.cjrm.XY19070031
21. **Yuan, X., Guan, N., Hou, G.** Research Progress on Reliability and Preparation of High Temperature SolidSelf-lubricating Coatings *Materials Reports* 34 (3) 2020: pp. 05061 – 05067. https://doi.org/10.11896/cldb.18110171
22. **Tarel'nik, V.B., Paustovskii, A.V., Tkachenko, Y.G., Martsinkovskii, V.S., Konoplyanchenko, E.V., Antoshevskii, K.** Electric-Spark Coatings on a Steel Base and Contact Surface for Optimizing the Working Characteristics of Babbitt Friction Bearings *Surface Engineering and Applied Electrochemistry* 53 (3) 2017: pp. 285 – 294. https://doi.org/10.3103/S1068375517030140
23. **Wang, X., Long, W., He, P.** Effect of Aging Treatment on Interfacial Microstructure and Mechanical Properties of Ni/babbitt Alloy *Transactions of the China Welding Institution* 40 (8) 2019: pp. 113 – 117. https://doi.org/10.12073/j.hjxb.2019400218
24. **Kreivaitis, R., Žunda, A., Kupčinskas, A., Jankauskas, V.** A Study of Tribological Behaviour of W-Co and Cu Electro-spark Alloyed Layers under Lubricated Sliding Conditions *Tribology International* 103 2016: pp. 236 – 242. https://doi.org/10.1016/j.triboint.2016.07.010
25. **Tarelnyk, V., Martsynkovskiy, V., Konoplianchenko, I.** Electroerosive Alloying Modes Optimization at Formation of a Special Microrelief on Bronze Sliding Bearings Friction Surfaces Selected Problems of Mechanical Engineering and Maintenance *Wydawnictwo Politechniki Świętokrzyskiej* 188 2012: pp. 98 – 103.
26. **Tarelnyk, V., Martsynkovskyy, V.** Upgrading of Pump and Compressor Rotor Shafts Using Combined Technology of Electroerosive Alloying *Applied Mechanics and Materials* 630 2014: pp. 397 – 412. https://doi.org/10.4028/www.scientific.net/AMM.630.397
27. **Tarelnyk, V., Martsynkovskyy, V., Dziuba, A.** New Method of Friction Assemblies Reliability and Endurance Improvement *Applied Mechanics and Materials* 630 2014: pp. 388 – 396. https://doi.org/10.4028/www.scientific.net/AMM.630.388
28. **Wang, J., Wang, D., Wang, X.** Property Improvement of Tin-based Babbitt B83 Based on Metallography Control *Materials Science and Technology* 26 (5) 2018: pp. 89 – 96. https://doi.org/10.11951/j.issn.1005-0299.20170368
29. **Sbiaai, K., Eddiai, A., Boughaleb, Y., Hajjaji, A., Mazroui, M., Kara, A.** Ag adatom and dimer motion on Cu (110) (1 × 2) missing row surface *Optical Materials* 36 (1) 2013: pp. 42 – 46. https://doi.org/10.1016/j.optmat.2013.06.016
30. **Lai, K.C., Liu, D.J., Thiel, P.A., Evans, J.W.** Modeling of Diffusivity for 2D Vacancy Nanopits and Comparison with 2D Adatom Nanoislands on Metal (100) Surfaces Including Analysis for Ag (100) *Journal of Physical Chemistry C* 122 (21) 2018: pp. 11334 – 11344. https://doi.org/10.1021/acs.jpcc.7b12527
31. **Patnaik, L., Maity, S.R., Kumar, S.** Comprehensive Structural, Nanomechanical and Tribological Evaluation of Silver Doped DLC Thin Film Coating with Chromium Interlayer (Ag-DLC/Cr) for Biomedical Application *Ceramics International* 46 (14) 2020: pp. 22805 – 22818. https://doi.org/10.1016/j.ceramint.2020.06.048